

UNCLASSIFIED

AD **407 296**

DEFENSE DOCUMENTATION CENTER

FOR

SCIENTIFIC AND TECHNICAL INFORMATION

CAMERON STATION, ALEXANDRIA, VIRGINIA



UNCLASSIFIED

NOTICE: When government or other drawings, specifications or other data are used for any purpose other than in connection with a definitely related government procurement operation, the U. S. Government thereby incurs no responsibility, nor any obligation whatsoever; and the fact that the Government may have formulated, furnished, or in any way supplied the said drawings, specifications, or other data is not to be regarded by implication or otherwise as in any manner licensing the holder or any other person or corporation, or conveying any rights or permission to manufacture, use or sell any patented invention that may in any way be related thereto.

63-4-1

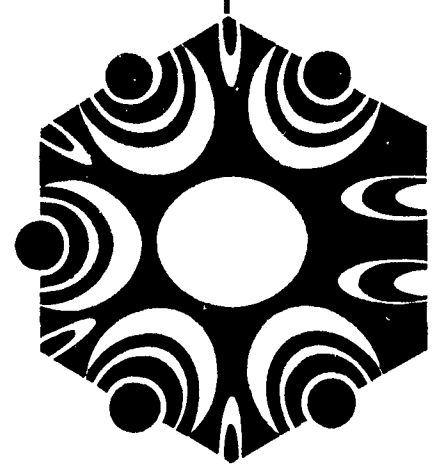
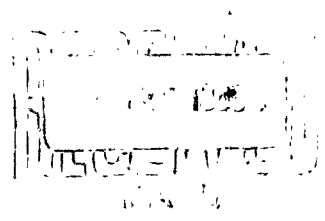
CATALOGED BY DDC
AS AD No. 407296

**SHEAR WAVE PROPAGATION IN A
BIREFRINGENT VISCOELASTIC MEDIUM**

407 296

by
George B. Thurston
and
John L. Schrag

June, 1963



**RESEARCH
FOUNDATION**

**OKLAHOMA STATE
UNIVERSITY**

Technical Report

Contract No. Nonr-2595(03)

Project No. 385-545

ONR Code 468

Shear Wave Propagation in a Birefringent Viscoelastic Medium

by

George B. Thurston, Principal Investigator

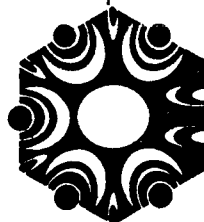
and

John L. Schrag, Graduate Research Assistant

June, 1963

This work was supported by Contract Number Nonr-2595(03), Project Number 385-545 between the Department of the Navy, ONR Code 468 and the Oklahoma State University. Reproduction in whole or in part is permitted for any purpose of the United States Government.

**ACOUSTICS LABORATORY
PHYSICS DEPARTMENT**



**RESEARCH
FOUNDATION**

OKLAHOMA STATE
UNIVERSITY, STILLWATER

SHEAR WAVE PROPAGATION IN A BIREFRINGENT

VISCOELASTIC MEDIUM

by

George B. Thurston and John L. Schrag

Department of Physics, Oklahoma State University

Stillwater, Oklahoma

ABSTRACT

A theoretical and experimental study is described for the optical birefringence associated with the propagation of a plane shear wave in a viscoelastic medium. The shear wave propagation is characterized by a complex propagation constant from which the complex coefficient of shear viscosity of the medium may be derived. The optical birefringence is related to the mechanical action of the shear wave by a complex mechano-optic coefficient. In the experiment the birefringence due to the shear wave is analyzed by transmitting circularly polarized light through the material at right angles to the direction of shear wave propagation and to the direction of particle displacement. The modified circularly polarized light is then analyzed by a plane analyzer and a photomultiplier detector. The mechanical and mechano-optic constants for the medium are determined for an aqueous milling yellow solution and for a polystyrene solution and are compared with independent determinations of these same factors from other experiments.

INTRODUCTION

An interesting combination of effects is involved in the study of shear wave propagation in viscoelastic birefringent media. First, the characteristics of the shear waves are dependent upon the combined viscous and elastic character of the medium, which may be either in the liquid or solid forms. These waves are rather rapidly attenuated but not so rapidly as to disguise their true wave character. Second, the shearing action of the wave may induce an optical birefringence of sufficient magnitude as to render the entire progressive wave pattern visible for purposes of detailed examination. Thus, these combined effects provide a situation where a precise study of the propagation of an attenuated wave may be carried out and the results related to the fundamental viscoelastic mechanical properties of the medium as well as to the optical effects of the mechanical action. Finally, it is particularly significant that by these studies the complex mechano-optic coefficient S^* and the complex viscosity coefficient η^* may be determined from a single experiment and thereby offer the opportunity of direct observation of the possible interrelations between these factors. As other methods have been developed for determination of S^* ¹ and η^* ^{2,3,4} separately, it is also well to utilize this experiment as a means of independent verification of the validity of these methods. While the conditions of determinations of S^* and η^* using a small sample of material confined to a small volume may lead to values appropriate to isothermal conditions, the analysis of wave propagation experiments generally gives adiabatic constants.⁵ Though the difference may be small,⁶ comparison of experimental results is of value in such cases.

In most previous work on shear wave propagation in birefringent media, the optical effect has been used only as an indicator for the purpose of deduction of mechanical properties. Using a visual technique Ferry⁷ has studied the shear wave propagation in gels, the method later being extended to the study of substances of high molecular weight.⁸ Further details of the effects of finite dimensions of the generating plane and fluid filled tanks used in the experiment were considered by Adler, Sawyer, and Ferry.⁹ Carrelli and Branca¹⁰ used the optical effect in a colloid to measure the shear wavelength. Penkov¹¹ carried out measurements of the velocity and attenuation by a visual technique and then sought to compute a Maxwell optical constant for castor oil, treating the wave propagation as for a Stokes viscous fluid and the optical effect as in steady flow determinations. Later, Penkov¹² carried out similar measurements on polymer solutions using a photo-multiplier for detection of the optical effect.

In the work to be described herein, results of determination of the two components of the complex mechano-optic coefficient and the two components of the complex viscosity coefficient for an aqueous solution of milling yellow N.G.S., a dye product from Allied Chemical and Dye Corporation, and for polystyrene in a polychlorinated polyphenyl solvent, Aroclor, from the Monsanto Chemical Corporation.

THEORETICAL DEVELOPMENT

A. Plane Shear Wave in a Viscoelastic Medium

The details of the theory of propagation of a plane shear wave have been described elsewhere.^{13,14} As used in this work, the form of the

relation between the shearing stress and the time rate of shear strain for sinusoidal motions is

$$\tau = \eta^*(\partial \dot{\xi} / \partial x) \quad (1)$$

where τ is the shear stress, $\dot{\xi}$ is the time rate of shear displacement, and η^* is the complex coefficient of shear viscosity. It is assumed that $\dot{\xi}$ is a function of the single space coordinate, x , and time, t , only.

Combining (1) with the Newtonian equation of motion, gives the one dimensional wave equation

$$\eta^*(\partial^2 \dot{\xi} / \partial x^2) = \rho(\partial \dot{\xi} / \partial t) \quad (2)$$

where ρ is the density of the medium. Taking the solution for propagation of a plane wave in the (+x) direction,

$$\dot{\xi} = \dot{\xi}_0 \exp[i(\omega t - \gamma x)] \quad (3)$$

gives

$$\gamma^2 = -(i\omega\rho)/\eta^* \quad (4)$$

where the complex propagation factor ($\gamma = \beta - i\alpha$), β being the phase factor ($\beta = \omega/v$, v being the propagation velocity) and α being the attenuation factor. If this wave is generated by a rigid plane, oscillating in its own plane, and this plane is located at $x = 0$, then from (3) it is seen that $\dot{\xi}_0$ is the amplitude of motion of the surface generating the plane wave.

The phase and attenuation factors may be obtained from (4) by using the relations

$$\begin{aligned} \eta^* &= \eta' - i\eta'' \\ &= \eta \exp(-i\varphi). \end{aligned} \quad (5)$$

The result is

$$\begin{aligned} \beta &= (\rho\omega/\eta)^{\frac{1}{2}} \cos[(\varphi/2) - (\pi/4)] \\ \alpha &= -(\rho\omega/\eta)^{\frac{1}{2}} \sin[(\varphi/2) - (\pi/4)] \end{aligned} \quad (6)$$

and, the inverse relations are

$$\eta = (\rho\omega)/(\alpha^2 + \beta^2) \quad (7)$$

$$\tan \varphi = \frac{1}{2}[(\beta/\alpha) - (\alpha/\beta)].$$

B. Optical Birefringence and the Mechano-Optic Relation

The effect of the plane shear wave is to render the medium optically anisotropic. This anisotropy may be detected by the observation of the modification of polarization characteristics of light on transmission through the medium. For visual observation it is customary to utilize a plane polarizer and plane analyzer, crossed, and with polarization direction parallel to the generating plane surface, the optical transmission being at right angles to both the surface motion and the direction of shear wave propagation. By use of stroboscopic illumination, detailed visual analysis of the wave propagation may be carried out if the amount of birefringence is sufficient to give prominent field patterns.¹⁵

For more direct quantitative measurement, the stroboscopic light source may be replaced by a steady source of collimated light and the eye by a photomultiplier with appropriate baffling to give a very narrow angle of acceptance. In this way an electrical signal is produced which is susceptible to direct quantitative analysis.¹ Thus wave propagation characteristics may be studied for media having insufficient optical anisotropy for visual observation. For a small amount of birefringence, the crossed plane polarizers give rise to a dominant electric signal at twice the frequency of the shear wave. It is found that by substitution of circularly polarized light in place of the incident plane polarized light, an electrical signal is obtained having the fundamental frequency. Further, the amplitude is enhanced over that of the second harmonic

of the other scheme. In view of this advantage, this scheme is preferred for photoelectric measurement.

Figure 1 shows the elements of the optical system. The plane polarizer and quarter wave plate serve to produce right circular polarization of the transmitted monochromatic light, the electric vector for which is \vec{E} . The light then passes through the viscoelastic, birefringent medium which supports the plane shear wave propagating in the (+x) direction. Thus the directions of optical transmission, shear wave propagation, and fluid displacement are mutually perpendicular.

The orthogonal unit vectors \vec{u}_1 and \vec{u}_2 specify the preferred optical directions in the birefringent medium, the associated complex optical propagation factors being χ_1 and χ_2 , respectively. The light thus traverses a thickness, L , of birefringent medium and then passes through a plane analyzer having a transmission direction of the unit vector \vec{u} . The final transmitted electric vector is \vec{E}_t , the effects of which are ultimately detected by the photomultiplier.

The electric vector for the right circularly polarized light incident upon the birefringent fluid may be resolved into components directed in the \vec{u}_1 and \vec{u}_2 directions. Thus the electric vector is given by the real part of

$$\vec{E} = (\vec{u}_2 + \vec{u}_1 i)E \quad (8)$$

where

$$E = E_0 \exp[i(\omega t - \chi r)] \quad (9)$$

and χ is the propagation factor for free space, i.e., $(2\pi/\lambda)$ where λ is the free space wavelength. Neglecting more complicating features¹⁶ at the interfaces on entering and leaving the birefringent fluid, it is assumed that the \vec{u}_1 and \vec{u}_2 components of (8) propagate through the fluid

in a manner characterized by the propagation factors χ_1 and χ_2 . Having thus propagated a distance, L , the emerging electric vector, \vec{E}' , is

$$\vec{E}' = [\vec{u}_2 \exp(-i\chi_2 L) + \vec{u}_1 i \exp(-i\chi_1 L)] \vec{E}. \quad (10)$$

Only the \vec{u} component of \vec{E}' is transmitted by the analyzer, thus

$$\vec{E}_T = \vec{u} E_T \exp[i(\omega t - \chi r)] \quad (11)$$

where

$$E_T = E_0 [\cos(\theta - \Psi) \exp(-i\chi_2 L) + i \sin(\theta - \Psi) \exp(-i\chi_1 L)] \quad (12)$$

The photomultiplier response is proportional to the magnitude of the Poynting vector as incident upon the photocathode. Thus, the factor of interest is the average value of the optical energy flow per cycle passing through an area normal to the propagation direction of the plane polarized wave (11). The photo response is then proportional to the factors as follows,¹⁷

$$I \propto \vec{w} \cdot (\vec{E}_T \vec{E}_T^*) \quad (13)$$

where \vec{w} is a unit vector in the direction of optical transmission. The complex conjugate E_T^* is obtained from (12) as

$$E_T^* = E_0 [\cos(\theta - \Psi) \exp(i\chi_2^* L) - i \sin(\theta - \Psi) \exp(i\chi_1^* L)]. \quad (14)$$

Substitution into (13) gives

$$I \propto \vec{w} \cdot E_0^2 \{ \cos^2(\theta - \Psi) \exp[i(\chi_2^* - \chi_2)L] + \sin^2(\theta - \Psi) \exp[i(\chi_1^* - \chi_1)L] \\ + i \cos(\theta - \Psi) \sin(\theta - \Psi) [\exp[i(\chi_2^* - \chi_1)L] - \exp[i(\chi_1^* - \chi_2)L]] \}. \quad (15)$$

At this point it is expedient to assume that the space rate of attenuation of the optical components is the same for the \vec{u}_1 and \vec{u}_2 directions. Thus neglecting possible dichroic effects, we have

$$\left. \begin{aligned} \chi_1 &= \kappa_1 - i\mu \\ \chi_2 &= \kappa_2 - i\mu \\ \chi_1^* &= \kappa_1 + i\mu \\ \chi_2^* &= \kappa_2 + i\mu \end{aligned} \right\} \quad (16)$$

Substitution into (15) gives

$$I \propto \vec{w} [E_0 \exp(-\mu L)]^2 \{1 + 2 \cos(\theta - \psi) \sin(\theta - \psi) \sin[(\mu_1 - \mu_2)L]\}. \quad (17)$$

It is seen that under the condition that the analyzer orientation is such that \vec{u} is parallel to either \vec{u}_1 or \vec{u}_2 , then $(\theta - \psi) = (0 \text{ or } \pi/2)$ and the photoresponse is

$$I_0 \propto \vec{w} [E_0 \exp(-\mu L)]^2. \quad (18)$$

This same photoresponse is obtained if the medium is not birefringent and $(\mu_1 - \mu_2 = 0)$. These special situations then offer the possibility of an experimental determination of the several factors which establish I_0 .

Equation (17) may be written in terms of the relative retardation, by noting

$$(\mu_1 - \mu_2)L = (2\pi/\lambda)\delta \quad (19)$$

where

$$\delta = (n_1 - n_2)L, \quad (20)$$

n_1 and n_2 being the optical indices of refraction associated with the directions \vec{u}_1 and \vec{u}_2 . Making use of (18) and (19) in equation (17) then gives the photoresponse as

$$I = I_0 [1 + k \sin(2\pi\delta/\lambda)] \quad (21)$$

where

$$k = 2 \cos(\theta - \psi) \sin(\theta - \psi). \quad (22)$$

C. Shear Wave Induced Birefringence

The relation between the birefringence and the shearing action for sinusoidal motion in the medium must take into account both relative magnitudes and phase relations which may exist between the amount of birefringence and the time rate of strain. Though one could as well establish such a relation between birefringence and shear stress, it would be simply related to that in terms of the time rate of strain by

the complex viscosity coefficient η^* . The relation which has been used for liquids¹ is

$$(n_1 - n_2)^* = -S \exp(i\theta_s) (\partial \dot{\xi} / \partial x) \quad (23)$$

where S and θ_s are the magnitude and phase of the complex mechano-optic coefficient S^* , and, for the relatively simple deformations of this work, the rate of strain is simply the velocity gradient $(\partial \dot{\xi} / \partial x)$. The velocity gradient for the plane shear wave (3) is

$$(\partial \dot{\xi} / \partial x) = \dot{\xi}_0 (\beta^2 + \alpha^2)^{1/2} \exp(-\alpha x) \exp[i(\omega t - \beta x - \pi/2 - \arctan(\alpha/\beta))]. \quad (24)$$

By combining (23) and (24) a complex relative retardation δ^* may be formed from (20). It is necessary to take the real part of this for substitution into the photocurrent equation. Thus, the retardation is

$$\delta = \delta_m \cos(\omega t + \sigma) \quad (25)$$

where

$$\delta_m = SL\dot{\xi}_0 (\beta^2 + \alpha^2)^{1/2} \exp(-\alpha x) \quad (26)$$

and

$$\sigma = -\beta x + \pi/2 - \arctan(\alpha/\beta) + \theta_s. \quad (27)$$

Thus it is seen that at a given location x in the fluid, the retardation is sinusoidally time varying at the frequency of the shear wave. Substitution of (25) into (21) gives the photoresponse

$$I = I_0 \{1 + k \sin[(2\pi/\lambda)\delta_m \cos(\omega t + \sigma)]\}. \quad (28)$$

For ease of analysis of experimental data it is preferable to specialize (28) to cases for sufficiently small retardation that

$$\sin(2\pi\delta/\lambda) \cong (2\pi\delta/\lambda). \quad (29)$$

To the precision of related experimental observations, this is generally applicable for $(\delta < \lambda/12)$. Subject to this approximation, (28) becomes

$$I \cong I_0 + I_1 \cos(\omega t + \sigma) \quad (30)$$

where

$$I_1 = I_0 k(2\pi/\lambda)\delta_m. \quad (31)$$

Taking the extreme condition of ($\delta_m = \lambda/12$) and the orientation factor ($k = 1$) gives a maximum value to the ratio (I_1/I_0) for validity of (30) as (0.524). Under usual conditions of experiment it is found that ($\Psi = 45^\circ$) and ($\theta - \Psi$) is set at 45° , thus ($k = +1$).

Figure 2 demonstrates the occurrences at a location in the shear wave field for ($k = +1$). Shown are the velocity of motion, $\dot{\xi}$, of the wave generating plane located at ($x = 0$) and the particle velocity at a field location, x . The relative retardation, δ , at the field location is shown and the phase angle σ is noted. The photoresponse, I , varies around the quiescent value I_0 and preserves the sinusoidal waveform if the limits of valid approximation are not exceeded. However, if the maximum value of the relative retardation is increased to a value, ($\delta_m = \lambda/4$), then the photoresponse will range from 0 to $2I_0$, but lose sinusoidal character. For larger δ_m , all photoresponses are confined to these same limits.

Finally it is interesting to note the relations between the characteristics of the propagating waves of velocity gradient, stress, birefringence, relative retardation, and photoresponse. From (1), (23), (24), (25), and (30) and using complex representations, it is seen that

$$\frac{\partial \dot{\xi}}{\partial x} = \frac{\tau}{\eta^*} = \frac{\Delta n}{S^*} = \frac{\delta}{S^*L} = \frac{(I - I_0)}{S^*(2\pi L/\lambda)}. \quad (32)$$

Thus the waves of the several factors in the numerators differ in phase by amounts associated with the angles of the denominators but all propagating and attenuating at the same rate.

D. Summary for Analysis of Experimental Data

Aside from the density of the medium and the orientation angle Ψ , the material constants which are essential to the description of the propagation of birefringence are those of the complex coefficient of viscosity, η and φ , and those of the mechano-optic coefficient, S and θ_s . With these constants, the photoresponse to the shear wave induced birefringence may be computed using (28). Conversely, from the observed photoresponse, the material constants may be determined. A convenient procedure is based on observations for small relative retardations for which the equation (30) is applicable.

In the experiment, the analyzer is rotated to a position which extinguishes the first harmonic photoresponse, I_1 , thereby determining the angle Ψ . Then, the normal condition of operation is set for ($k = +1$), and by appropriate instrumental methods, measurement of the amplitude and phase of the first harmonic, I_1 and σ , as a function of the shear wave propagation distance x is carried out. The quiescent photoresponse, I_0 , and the velocity amplitude of the generating plane surface, $\dot{\xi}_0$, are also observed.

From (26) and (31) it is seen that

$$[I_1 / (I_0 \dot{\xi}_0)] = [(2\pi kSL/\lambda)(\beta^2 + \alpha^2)^{1/2}] \exp(-\alpha x). \quad (33)$$

Thus, from the experimental observations, a plot is formed of $\log [I_1 / (I_0 \dot{\xi}_0)]$ vs. x as the experimental equivalent of (33). Also, observed values of σ vs. x are plotted for the experimental equivalent of (27). Thus from the slope of the $\log [I_1 / (I_0 \dot{\xi}_0)]$ curve, α may be determined, while from the slope of the σ curve, β may be determined. By extrapolation of the experimental observations to the plane, ($x = 0$),

values of $[(2\pi kSL/\lambda)(\beta^2 + \alpha^2)^{\frac{1}{2}}]$ and $[\pi/2 - \arctan(\alpha/\beta) + \theta_s]$ are obtained, which, by introduction of the measured values of α and β and the other factors, will then yield S and θ_s . Also, η and φ may be computed from α and β by equation (7).

EXPERIMENTAL EVALUATION

A. Apparatus

Figure 3 shows a diagram of the apparatus developed. The illumination is provided by a tungsten lamp L and collimator assembly C, the lamp illuminating a small circular aperture which acts as the source for the collimator. The collimated beam, which is 5 cm in diameter, is filtered by a Bausch and Lomb 5790 Å interference filter IF. A Polaroid polarizer P and quarter wave plate ($\lambda/4$) combination provides the right circularly polarized light which is incident upon the fluid cell FC. A Polaroid analyzer A follows the fluid cell. The light transmitted by the analyzer is incident upon the photomultiplier-slit system, PH, in which two adjustable vertical slits separated by approximately 4 inches define the light beam reaching the photocathode of the photomultiplier tube. The front slit reduces the effect of general background illumination, while the narrower rear slit serves principally as the defining slit which determines the surface area of the fluid cell over which the emerging light is summed by the photocathode.

The brass driving plane PL generating the shear wave is 4.0 cm along the optical path and is immersed approximately 5 cm in the liquid. The brass fluid cell has glass windows which give a cross sectional view of the entire test medium. In the cell, the fluid depth is 5.6 cm,

the optical path is 4.2 cm, and the width in the direction of shear wave propagation is 5.0 cm. The fluid cell is fitted with a brass cap which is in contact with the fluid in the region of study and is for the purpose of damping surface waves. The shaft supporting the plane PL is guided in the mechanism of the electrodynamic driver D by two cylindrical bearings spaced approximately 5 inches apart. A bellows connecting the drive shaft to the body of the driver serves both as a spring support and as a constraint against rotation of the shaft during translation. The velocity of motion of the drive shaft and plane is monitored by means of the electrodynamic unit VM.

The outputs of the photomultiplier and the velocity monitor are displayed on a dual trace cathode ray oscilloscope for general monitoring, while their amplitudes and phases are measured with an electronic wave analyzer and an electronic phase meter. The position of the photomultiplier is determined by the traveling micrometer stage T. The steel frame supporting the driver, traveling stage, and fluid cell weighs approximately 60 pounds. An additional 65 pounds of mass is attached to the base of the frame for further reducing motions of the over-all structure. The remaining elements of the optical system are attached to a rigid supporting structure for preserving the precise optical alignment required. The lamp to photomultiplier distance is then approximately 35 inches.

Visual observation of the shear wave field shows the general propagation characteristics of the shear wave as well as some of the influences of the various cell components on the shear wave field pattern. Figure 4 shows a photograph of the fluid cell FC with cap block B in place, the oscillating plane PL and holder H. The instantaneous shear

wave field pattern is for milling yellow using crossed Polaroids and unfiltered stroboscopic illumination. For such a white light source, the spacing between black zero order fringes in a reflection free region is one half the shear wavelength. The remaining fringes near the plane are colored. The plane is positioned to the left of the cell and measurements are carried out to the right of the plane where a greater propagation range is possible, thus minimizing wall reflection. The decreasing intensity of illumination with distance of propagation demonstrates the attenuation of the wave as it propagates out from the plane. Note that the presence of the cell cap block makes the pattern on the right of the plane symmetric whereas the pattern on the left is not. The measurements are made in the region near the driving surface for which the wave surfaces are most nearly plane.

The photocurrent equation (28) was shown to exhibit a sinusoidal character for retardations of less than one twelfth of a wavelength, but to deviate from this simple character for larger retardations. Figure 5 illustrates four of these photocurrent waveforms as obtained from photographs of the oscilloscope face using a milling yellow solution at 22 cps with 5790 \AA illumination. The four traces were taken for a fixed value of x and demonstrate the change in waveform with drive amplitude. The first trace (0db) shows the sinusoidal character of the waveform for $\delta_m < \lambda/12$, the second (10db) shows the waveform for δ_m slightly greater than $\lambda/4$, the third (15db) shows the waveform for δ_m between $\lambda/2$ and $\frac{3}{4}\lambda$, and the fourth (20db) shows the waveform for δ_m approximately equal to λ . The waveforms demonstrate the trace characteristics of equation (28) except for the narrowing of the trace for retardations greater than half a wavelength. For such retardations the

trace no longer goes from the 0 to $2I_0$ levels predicted by equation (28), but narrows as the drive amplitude increases. The effect is even more pronounced with white light and wider photomultiplier slits.

B. Measurement Limitations

Satisfactory measurement conditions are obtained when the noise level is sufficiently low and the general wave propagation conditions are proper. First, the shear wave must propagate a sufficient distance from the plane so that measurements can be made for propagation distances greater than 1 mm. For points nearer to the plane both the magnitude and phasing of the photocurrent deviate from the normal extrapolation of the propagation curves into this region. Also, there is a rapid decrease in the light intensity for distances within 1 mm of the plane which seriously limits the photocurrent. Second, the shear wavelength must be great enough that the photomultiplier does not average over more than one twelfth of the shear wavelength. If this criterion is exceeded, the photocurrent waveform changes appreciably. Since the photomultiplier tube produces a noise voltage between .1 and 1 millivolt rms, the measured photovoltage should be at least 5 millivolts rms. The maximum illumination levels obtainable from the tungsten lamp are such that the defining slit of the photomultiplier unit must be at least .002 inch wide to achieve the minimum useful photovoltage. Thus the shear wavelength criterion together with this minimum usable slit width define a minimum working shear wavelength of approximately .05 mm, which in turn sets an upper limit for the useful frequency range for a given solution. Third, the shear wave attenuation rate must be such that no wall reflections interfere with the primary wave,

and the fluid depth must be sufficient so that plane wave surfaces are present for some region near the plane. Fourth, the plane width to shear wavelength ratio must be at least 2. For ratios less than 2 the measured wavelength as well as the measured phase change significantly. These last two criteria determine a lower limit for the useful frequency range for a given fluid. To determine whether or not a given solution will have mechanical and optical properties adequate for study by the shear wave propagation technique, the value of $I_1 / (I_0 \xi_0)$ at $x \approx 1$ mm may be calculated from equation (33) and compared to the lowest measurable value for the test apparatus. In view of the criteria just discussed, the apparatus described in this paper is such that $I_1 / (I_0 \xi_0)$ must be greater than .001 sec/cm.

The plane location is determined by scanning the field with the photomultiplier unit noting when the photomultiplier enters and leaves the plane shadow. This determines the plane center location and hence its surface location. This measurement is reproducible to within approximately $\pm .03$ mm. If the shear wavelength is too small, this may introduce an appreciable error. There is some error in the alignment of the plane in the field of collimated light. However, in view of the uncertainty in plane surface location, this error seems to be negligible. The measurement of fluid temperature as carried out in this work has a probable error of $\pm .3^\circ$ C.

C. Propagation Characteristics and Determinations of Mechanical and Mechano-Optic Factors

The propagation characteristics have been obtained for a 1.34% aqueous solution of milling yellow N.G.S. and a 2% solution of polystyrene in Aroclor using the measurement techniques for $\delta_m < \lambda/12$. For these

measurements, the plane width was 4.0 cm, the driving frequency was 22 cps, $\Psi = 45^\circ$, and $k = +1$. Figure 6 shows the measured values of $I_1/(I_0 \xi_0)$ and σ versus x for the milling yellow solution, and Figure 7 shows the same quantities for the polystyrene solution. It is seen that the decrease of amplitude and phase with increasing distance has the character described by the idealizations of the theoretical treatment, but with some deviations for x greater than 7 mm.

Table I shows a summary of determinations of the factors α , β , S , and θ_s from the wave propagation experiment and the factors η , ϕ , S and θ_s for other independent experiments. The quantities enclosed in parentheses are calculated from the primary results using equations described herein. The tabulated values are for 22 cps.

The milling yellow has a value of α of approximately $(1/3) \beta$ indicating a substantial elasticity, while the polystyrene has comparable values of α and β indicating only a small degree of elasticity. The shear wavelengths are quite different also, the wavelength in milling yellow being approximately $1/5$ of that in polystyrene. The milling yellow illustrates the behavior of a solution with a large optical sensitivity, a considerable degree of elasticity, and a rather small viscosity while the polystyrene illustrates the behavior of a solution of small optical sensitivity, a small degree of elasticity, and a rather large viscosity.

The table shows that the values of the various factors determined from the shear wave propagation data for the polystyrene solution agree to within experimental error with the values determined from the independent experiments. The values of some of these same factors obtained from the milling yellow propagation data do not agree as closely with the results obtained from the independent measurements, but the uncertainty in the temperature measurement noted previously combined with the strong

dependence of these factors on temperature for the milling yellow solutions could account for such disagreements. It should be noted that the calculations of η and S from equations (7) and (33) involve some enhancement of measurement errors, and hence the shear wave propagation experiment is of more value as a comparative independent experiment for the determination of S^* and η^* than as a precise technique for their measurement. However, the shear wave constants themselves are not subject to such cumulative error and are reproducible to within 2% for a given fluid.

D. Conclusion

It is seen from the experimental evaluation that the solutions studied do exhibit the propagation characteristics described by the accompanying theory. Moreover, the measured values of the various mechanical and mechano-optic constants agree to within experimental error with the same factors determined from independent experiments. Hence the shear wave experiment serves as an independent verification for these various experiments. Thus the study of shear wave propagation as well as the determination of the mechanical and optical factors is carried out satisfactorily in one single experiment.

Since the shear wave propagation is approximately adiabatic in character whereas the other techniques noted are more nearly isothermal, the comparison of results presented in Table 1 could indicate the possible magnitude of the effect of the differing thermal conditions on the measured quantities. However, since the experimental errors are sufficiently large to account for the differences displayed, it is felt that the thermal effects are probably smaller than what would be

indicated by the differences shown, so that these differences should be regarded only as setting upper limits for the thermal effects.

. ACKNOWLEDGMENT

This work was supported by the U. S. Army Research Office (Durham), and by the Office of Naval Research, U. S. Navy.

REFERENCES

- ¹G. B. Thurston and J. L. Schrag, Trans. Soc. Rheology VI, 325 (1962).
- ²See review articles in Rheology, Theory and Applications, F. R. Eirich, ed., Academic Press, New York (J. D. Ferry, Ch. 11, Vol II, 1958, and S. Oka, Ch. 1, Vol III, 1960.)
- ³G. B. Thurston, J. Acoust. Soc. Am., 33, 1091 (1961).
- ⁴M. H. Birnboim and J. D. Ferry, J. Appl. Phys. 32, 2305 (1961).
- ⁵See, for example, W. P. Mason, Piezoelectric Crystals and their Application to Ultrasonics, (D. Van Nostrand Co., New York, 1950.)
- ⁶John D. Ferry, Viscoelastic Properties of Polymers, (John Wiley and Sons, New York, 1961) see Ch. 5 sec. G.
- ⁷J. D. Ferry, Rev. Sci. Inst. 12, 79 (1941).
- ⁸J. N. Ashworth and John D. Ferry, J. Am. Chem. Soc. 71, 622 (1949).
- ⁹F. T. Adler, W. M. Sawyer, and John D. Ferry, J. Appl. Phys. 20, 1036 (1949).
- ¹⁰A. Carrelli and G. Branca, Nuovo Cim. 8, 889 (1951).
- ¹¹S. N. Penkov, Optika i Spektroskopiya I, 77 (1956).
- ¹²S. N. Penkov, Optics and Spectroscopy (U.S.A.) 10, 343 (1961).
- ¹³Turner Alfrey, Jr., and E. F. Gurnee, "Dynamics of Viscoelastic Behavior", in Rheology, Theory and Applications, edited by F. R. Eirich (Academic Press, Inc., New York, 1958) Vol. I, Chap. 11.
- ¹⁴John D. Ferry, Viscoelastic Properties of Polymers (John Wiley and Sons, Inc., New York, London, 1961) pp. 93-97.
- ¹⁵L. E. Hargrove and G. B. Thurston, J. Acoust. Soc. Am. 29, 966 (1957).
- ¹⁶F. I. Federov, and T. L. Kotyash, Optics and Spectroscopy (U.S.A.) 12, 162 (1962).
- ¹⁷See for example, J. A. Stratton, Electromagnetic Theory (McGraw-Hill Book Company, Inc., New York and London, 1941) pp 131-137.
- ¹⁸Private communication from Professor John D. Ferry, University of Wisconsin.

TABLE 1

Summary of propagation factors, mechanical properties, and mechano-optic properties of 2% polystyrene in Aroclor and 1.34% aqueous milling yellow solution at a frequency of 22 cps. The factors in parentheses are computed using equations given in the text.

Material	Method	Temp.	α (1/cm)	β (1/cm)	η (poises)	φ	S (sec)	θ_s
2% Polystyrene in Aroclor	Shear Wave Propagation	23.6°C	2.68	2.95	(12.5)	(5.5°)	1.06×10^{-8}	-197°
	Dynamic Mechanical Method (J. D. Ferry ¹⁸)	25.0°C	(2.69)	(2.88)	12.1	7.1°		
	Thin Fluid Layer ¹⁾ (Thurston and Schrag)	23.7°C					1.15×10^{-8}	-186°
1.34% Milling Yellow N.G.S. in Water	Shear Wave Propagation	21.9°C	5.60	15.91	(.488)	(51.2°)	3.32×10^{-6}	-66°
	Oscillation in a Circular Tube (Thurston ³)	21.9°C	(6.50)	(15.82)	.478	45.3°		
	Thin Fluid Layer ¹⁾ (Thurston and Schrag)	21.0°C					3.21×10^{-6}	-69°

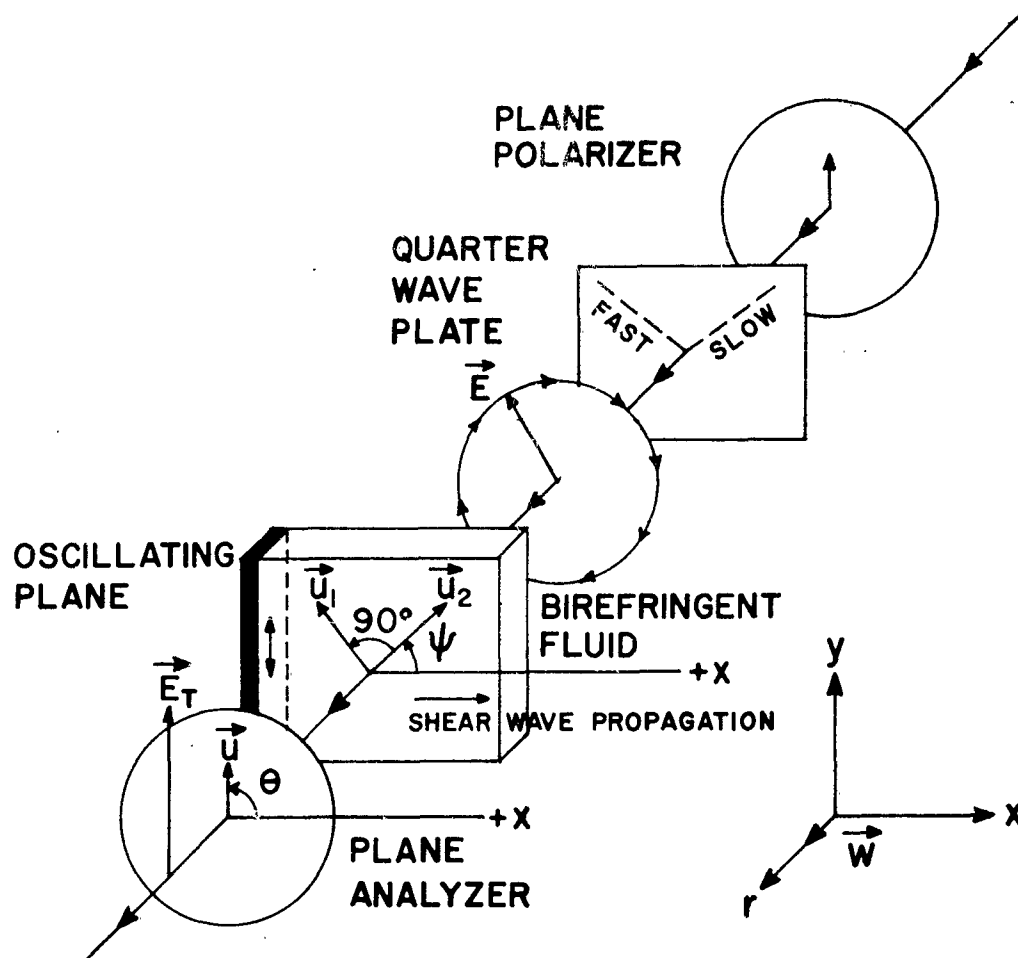


Figure 1. Arrangement of optical elements of the optical transmission system.

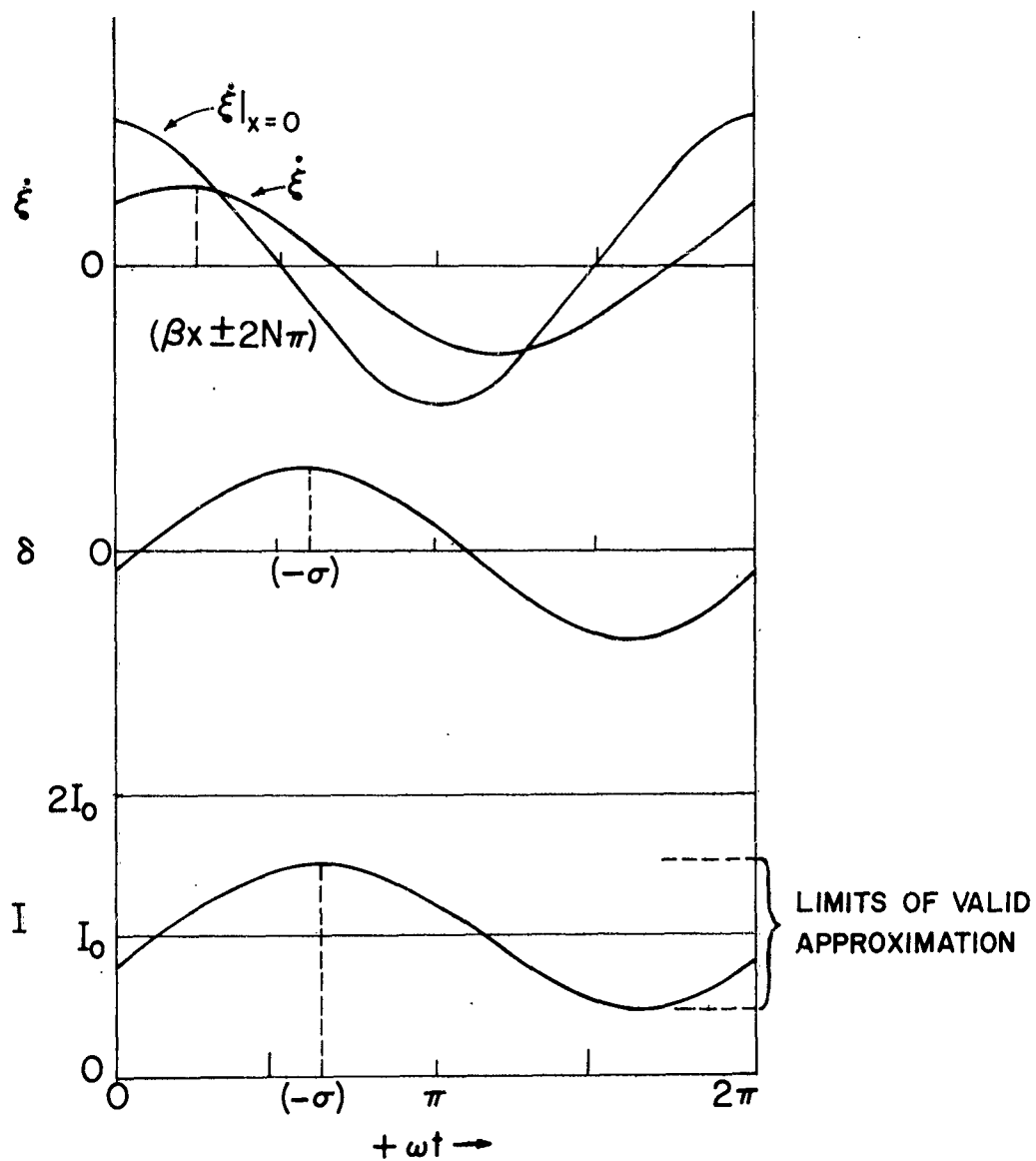


Figure 2. The velocity of the driving plane, and the velocity, retardation, and the photocurrent as a function of ωt at a fixed location in the fluid. The quiescent photocurrent I_0 , and the limits of valid approximation to the small retardation equation for $k = +1$ are indicated.

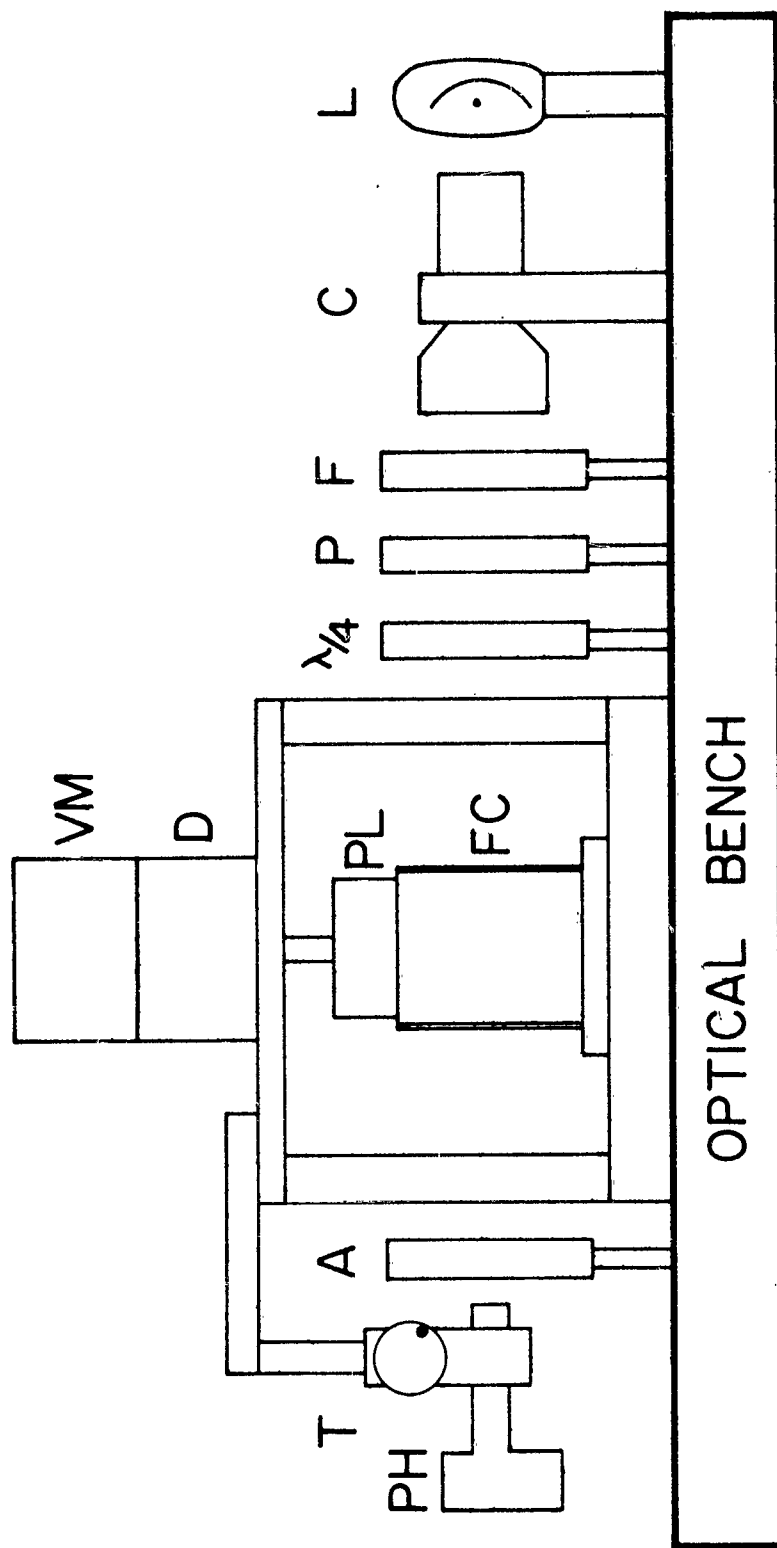


Figure 3. Diagram of the apparatus used for the shear wave propagation studies showing the light source L, the collimator C, the interference filter IF, the polarizer P, the quarter wave plate $\lambda/4$, the fluid cell FC, the oscillating plane PL, the driver D, the velocity monitor VM, the analyzer A, the traveling micrometer stage T, and the photomultiplier-slit assembly PH.

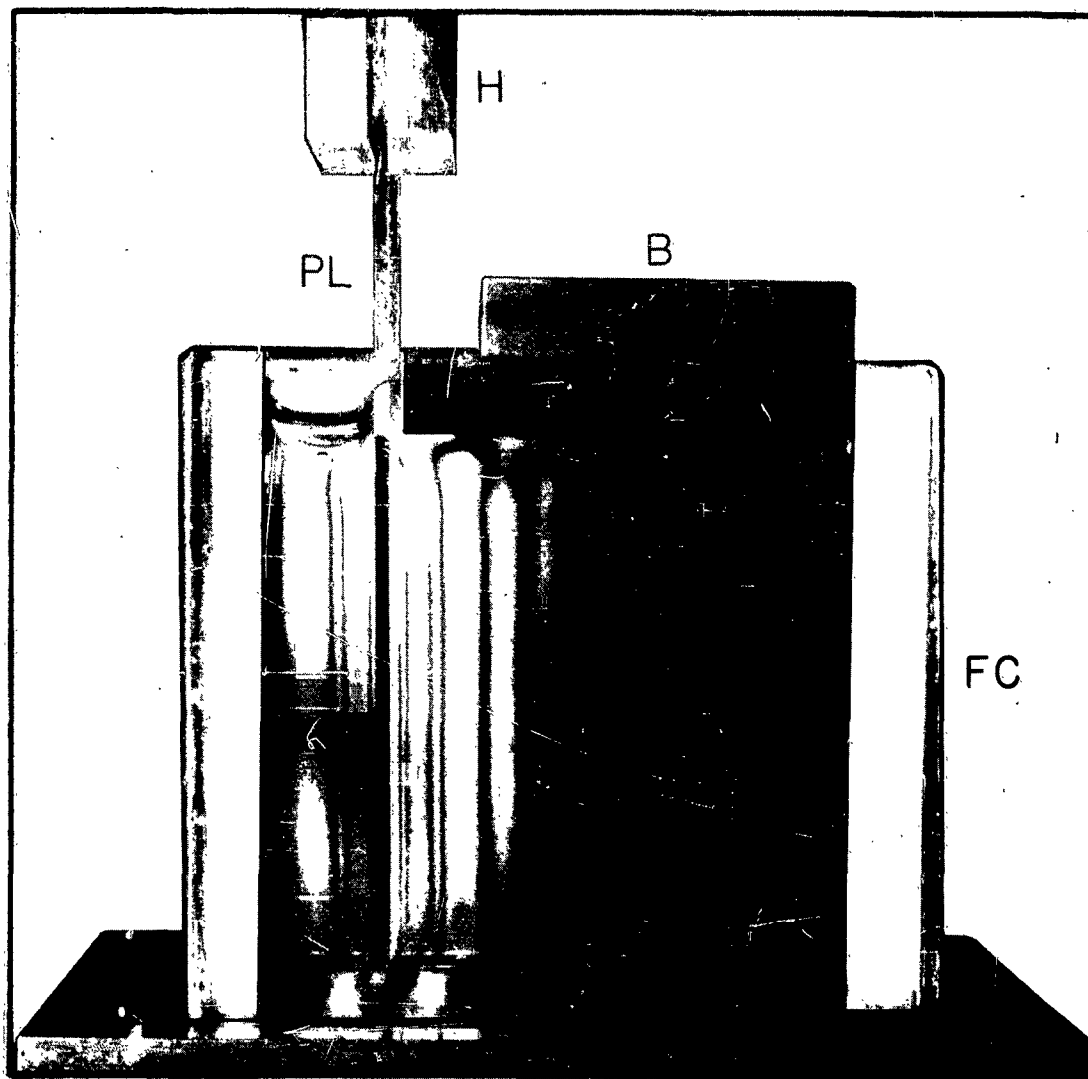


Figure 4. Photograph of the fluid test cell FC showing the oscillating plane PL and holder H, the cap block B, and a typical instantaneous shear wave field pattern for a milling yellow solution using white light illumination.

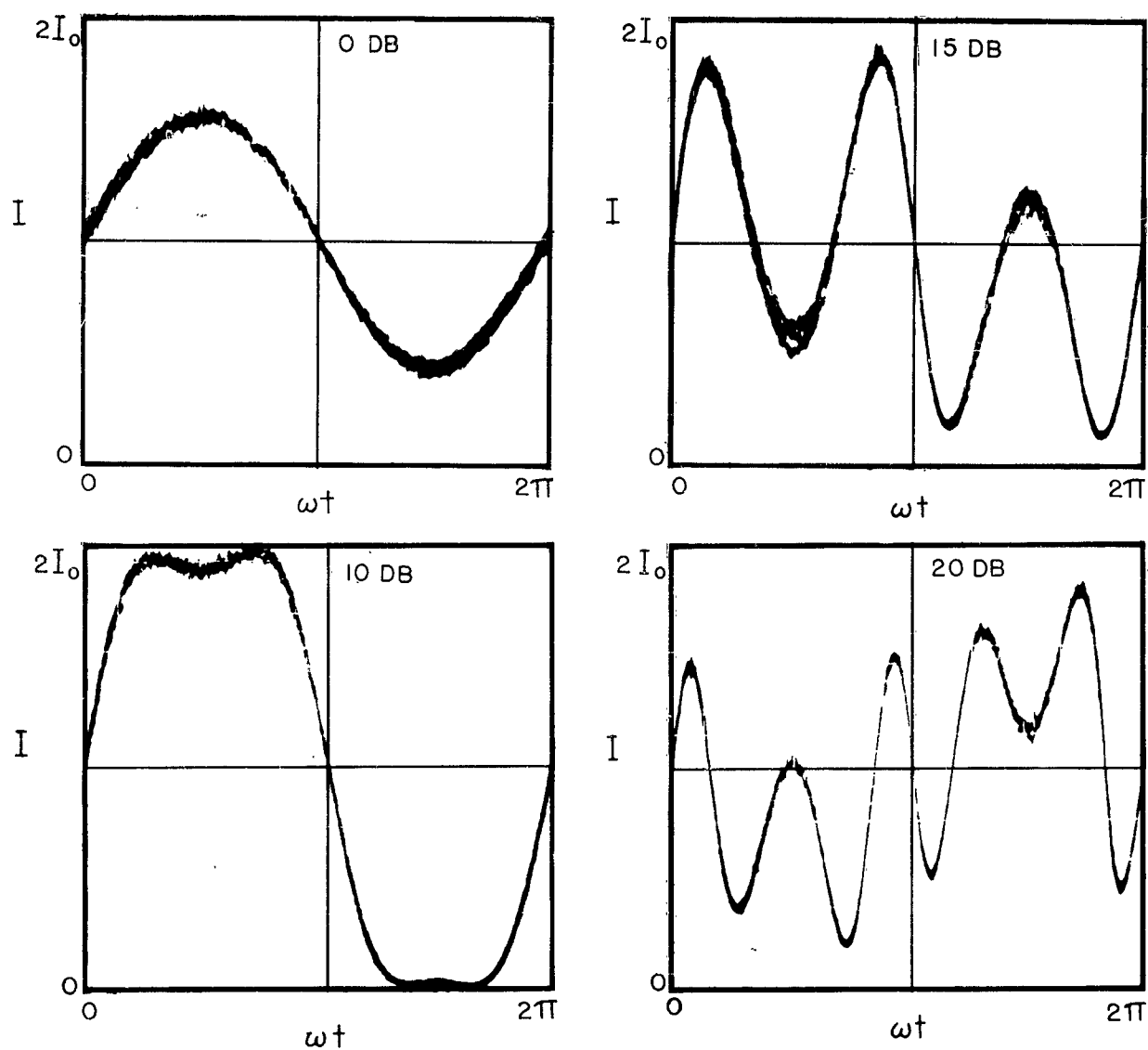


Figure 5. Experimental photocurrent traces obtained at a fixed field location for four different drive amplitudes. The relative decibel levels of the amplitude are as indicated.

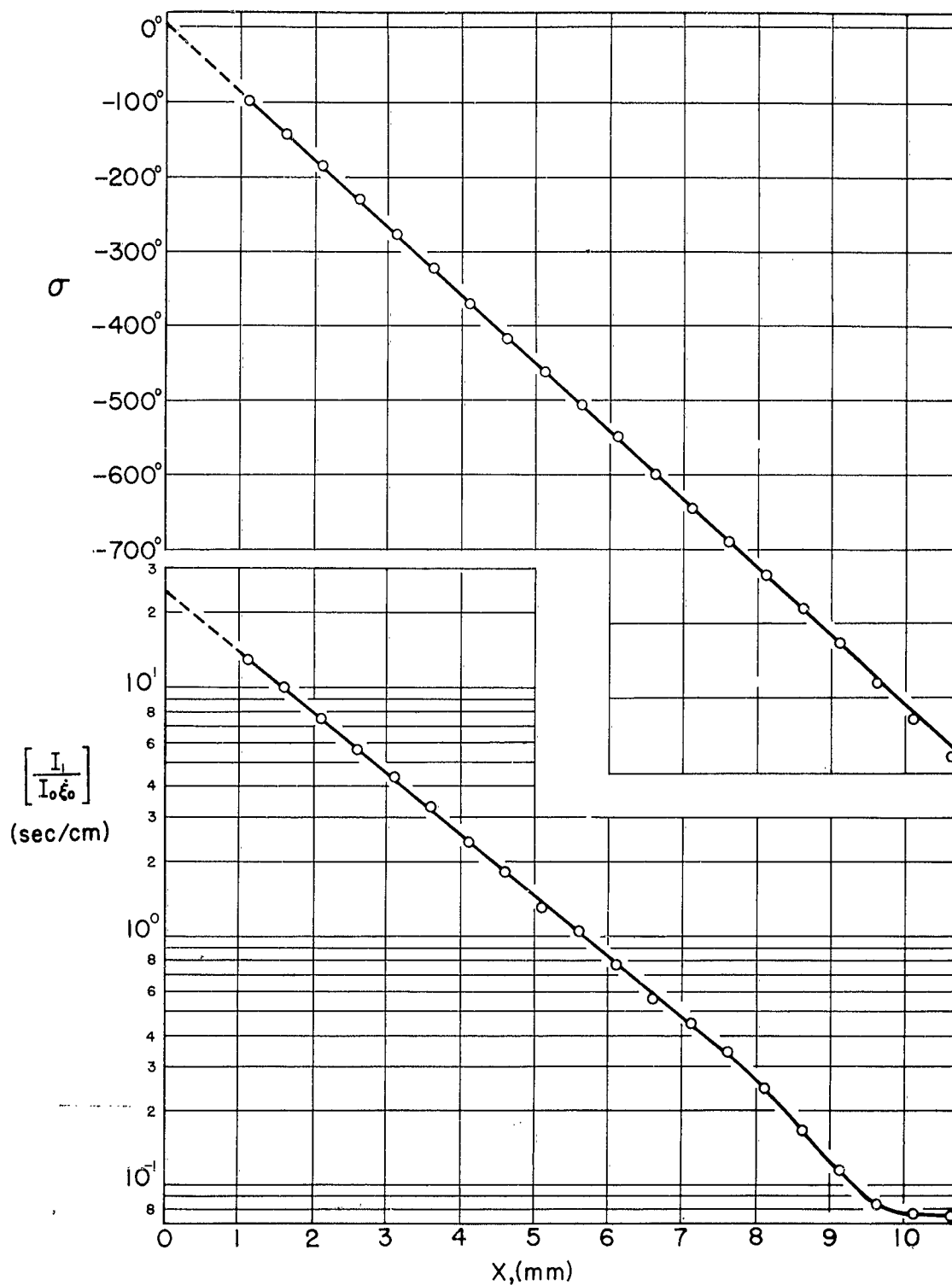


Figure 6. $\left[\frac{I_1}{I_0 \xi_0} \right]$ and σ Versus x for a 1.34% milling yellow solution at a driving frequency of 22 cps, a temperature of 21.9°C , and an optical wavelength of 5790 \AA .

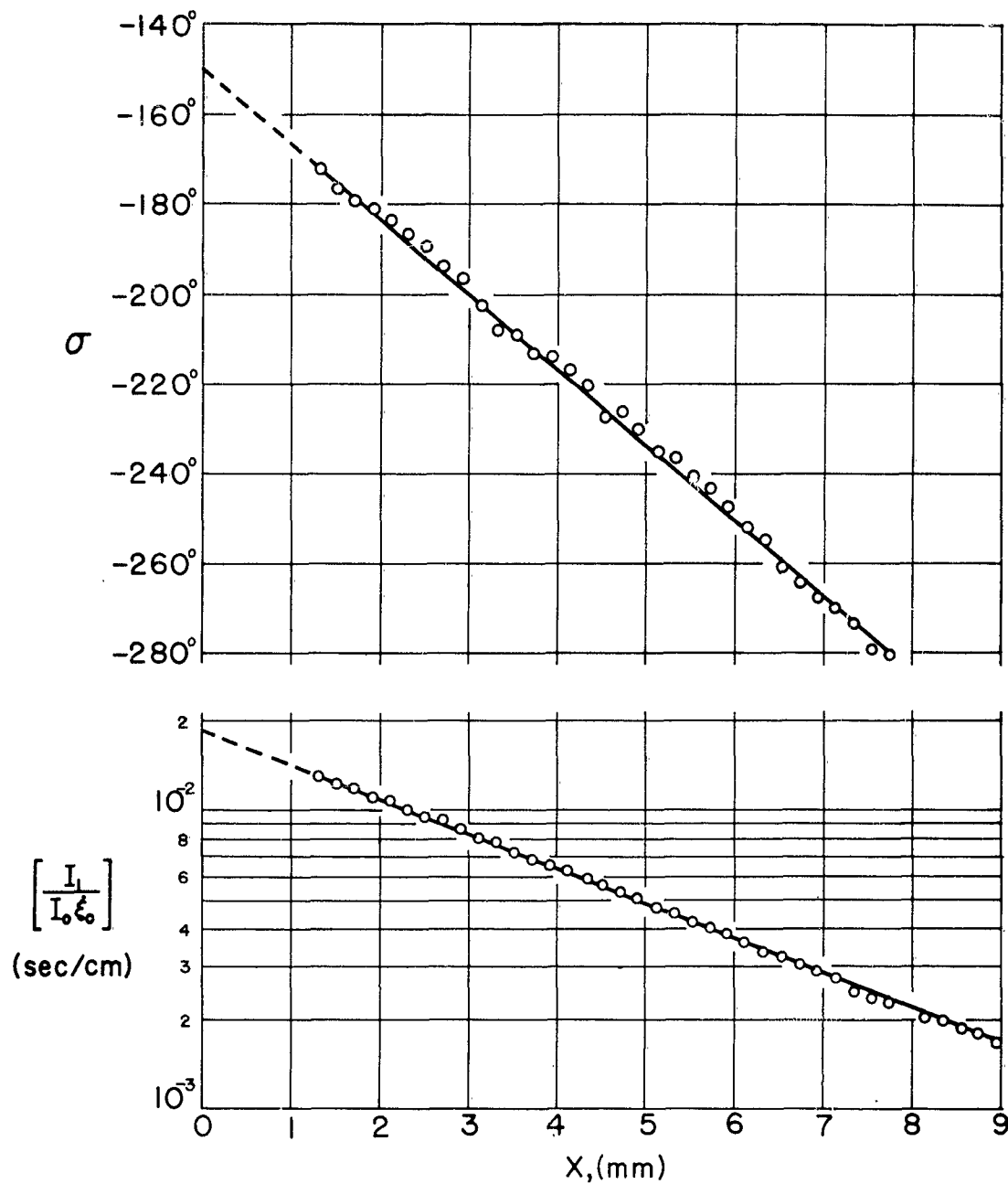


Figure 7. $\left[\frac{I_1}{I_0 \xi_0} \right]$ and σ versus x for a 2% polystyrene solution at a driving frequency of 22 cps, a temperature of 23.6°C , and an optical wavelength of 5790 Å.

Office of Naval Research (Code 468)
Department of the Navy
Washington 25, D. C. (2 copies)

Director
U. S. Naval Research Laboratory
Technical Information Division
Washington 25, D. C. (6 copies)

Director
U. S. Naval Research Laboratory
Sound Division
Washington 25, D. C. (1 copy)

Commanding Officer
Office of Naval Research Branch Office
The John Crerar Library Building
86 East Randolph Street
Chicago 1, Illinois (1 copy)

Commanding Officer
Office of Naval Research Branch Office
Box 39, Navy No. 100
FPO, New York, N. Y. (12 copies)

Armed Services Technical Information Agency
Arlington Hall Station
Arlington 12, Virginia (10 copies)

Commander
U. S. Naval Ordnance Laboratory
Acoustics Division
White Oak
Silver Spring, Maryland (1 copy)

Commanding Officer and Director
U. S. Navy Electronics Laboratory
San Diego 52, California (1 copy)

Director
U. S. Navy Underwater Sound Reference
Laboratory
Office of Naval Research
P. O. Box 8337
Orlando, Florida (1 copy)

Commanding Officer and Director
U. S. Navy Underwater Sound Laboratory
Fort Trumbull
New London, Connecticut (1 copy)

Commander
U. S. Naval Air Development Center
Johnsville, Pennsylvania (1 copy)

Director
National Bureau of Standards
Connecticut Avenue & Van Ness St., N.W.
Washington 25, D. C.
(Attn: Chief of Sound Section) (1 copy)

Office of Chief Signal Officer
Department of the Army
Pentagon Building
Washington 25, D. C. (1 copy)

Commanding Officer and Director
David Taylor Model Basin
Washington 7, D. C. (1 copy)

Superintendent
U. S. Navy Postgraduate School
Monterey, California
(Attn: Prof. L. E. Kinsler) (1 copy)

Commanding Officer
Air Force Cambridge Research Center
230 Albany Street
Cambridge 39, Mass. (1 copy)

Commanding Officer
U. S. Navy Mine Defense Laboratory
Panama City, Florida (1 copy)

U. S. Naval Academy
Annapolis, Maryland
(Attn: Library) (1 copy)

Chief, Physics Division
Office of Scientific Research
HQ Air Force Systems Command
Andrews AFB
Washington 25, D. C. (1 copy)

Harvard University
Acoustics Laboratory
Division of Applied Science
Cambridge 38, Mass. (1 copy)

Bureau of Naval Weapons
Code RU-222 (Oceanographer)
Washington 25, D. C.

Brown University
Department of Physics
Providence 12, R. I. (1 copy)

Director
Columbia University
Hudson Laboratories
145 Palisade Street
Dobbs Ferry, N. Y. (1 copy)

U. S. Navy SOFAR Station
APO #856, c/o Postmaster
New York, New York
(Attn: Mr. G. R. Hamilton) (1 copy)

B. F. Goodrich Research Center
Brecksville, Ohio
(Attn: Mr. Harry F. Neff) (1 copy)

Stanford Research Institute
Menlo Park, California (1 copy)

Chief Bureau of Ships
Department of the Navy
Washington 25, D. C.
(Attn: Code 688 (1 copy)
" " 345 (1 copy)
" " 634C (1 copy)

Defense Research Laboratory
University of Texas
Austin 12, Texas (1 copy)

Chief of Naval Research
Department of the Navy
Washington 25, D. C.
(Attn: Code 466 (1 copy)
" " 439 (1 copy)

Institute for Defense Analyses
Communications Research Division
Von Neumann Hall
Princeton, New Jersey